Published in final edited form as:
*Cell*. 2009 January 23; 136(2): 284–295. doi:10.1016/j.cell.2008.11.037.

# Age-dependent deterioration of nuclear pore complexes causes a loss of nuclear integrity in post-mitotic cells

**Maximiliano A. D'Angelo**, **Marcela Raices**, **Siler H. Panowski**, and **Martin W. Hetzer***
Salk Institute for Biological Studies, Molecular and Cell Biology Laboratory, 10010 N. Torrey Pines Road, La Jolla, 92037 CA, United States

## SUMMARY

In dividing cells, nuclear pore complexes (NPCs) disassemble during mitosis and reassemble into the newly forming nuclei. However, the fate of these multi-protein transport channels in post-mitotic cells, where the mitotic renewal of pores is absent, is unknown. Here we show that NPCs, unlike other nuclear structures, do not turn over in differentiated cells. While a subset of nuclear pore components, like Nup153 and Nup50, are continuously exchanged at the NPC, scaffold nucleoporins, like the Nup107/160 complex, are extremely long-lived and remain incorporated in the nuclear membrane during the entire lifespan of a cell. In addition to a lack of nucleoporin expression and NPC turnover, we discovered an age-related deterioration of NPCs leading to a loss of the nuclear permeability barrier and the leaking of cytoplasmic proteins into the nuclear compartment. Our finding that nuclear 'leakiness' is dramatically accelerated during aging and that a subset of nucleoporins are found to be oxidatively damaged in old cells, suggest that the accumulation of damage at the NPC structure might be a crucial event in age-related loss of nuclear integrity.

## INTRODUCTION

NPCs are large aqueous channels formed by the interaction of multiples copies of ~30 different proteins known as nucleoporins. Pores have an eight-fold symmetrical structure that consists of a nuclear envelope (NE)-embedded scaffold, which surrounds the central channel through which all nucleocytoplasmic transport occurs and a cytoplasmic and nuclear ring to which eight filaments are attached (Figure 1A). While the cytoplasmic filaments have one loose end, the nuclear filaments are attached to a distal ring forming a structure known as nuclear basket. NPCs span the double lipid bilayer of the NE at sites where the inner and the outer nuclear membranes are fused (Alber et al., 2007; Beck et al., 2004; Kiseleva et al., 2004; Reichelt et al., 1990). This unique membrane topology requires scaffold nucleoporins such as the Nup107/160 complex to stabilize the two fused membrane leaflets (Harel et al., 2003; Walther et al., 2003). To accommodate the selective transport of cargo across the NE, additional nucleoporins are attached to the membrane-embedded scaffold (Rabut et al., 2004a). Most of the peripheral nucleoporins, such as Nup153, contain FG-repeats, interact with nuclear transport receptors and provide a selective barrier for the diffusion of molecules larger than ~60 kDa (Rabut et al., 2004a; Weis, 2003).

In proliferating cells, the formation of new pores occurs during mitosis and interphase (D'Angelo et al., 2006; Maul et al., 1972; Rabut et al., 2004b) and requires the expression of the Nup107/160 complex members (Sec13, Seh1, Nup37, Nup43, Nup75, Nup96, Nup107, Nup133 and Nup160) (Harel et al., 2003; Walther et al., 2003), suggesting a general role for scaffold nucleoporins in establishing and maintaining the NPC structure. While most peripheral

*To whom correspondence should be addressed: hetzer@salk.edu, FAX 858-457-4765.

nucleoporins are constantly exchanged at the NPC, the pore scaffold is stable during interphase and only disassembles during the M-phase of dividing cells (Daigle et al., 2001; Rabut et al., 2004b). This raises the question of how the structural and functional integrity of NPCs is maintained throughout the life span of non-dividing cells where this mitotic renewal cycle is absent.

Using *C. elegans* and a mammalian differentiation system we found that the expression of the NPC scaffold members is strongly down regulated when the cells exit the cell cycle. Furthermore, we observed that the scaffold nucleoporins are extremely stable and do not exchange once they are incorporated into the NE, persisting for the entire life span of a differentiated cell. In addition, we discovered that in post-mitotic cells, NPCs deteriorate with time, losing nucleoporins responsible for maintaining the pore diffusion barrier. Strikingly, we found that nuclei of old rat neurons containing deteriorated NPCs show an increased nuclear permeability and the intranuclear accumulation of cytoplasmic tubulin. The findings that oxidative stress accelerates the age-related "leakiness" of pores and that the proteins that are lost from NPCs can be found carbonylated, a result of oxidative protein damage, in old cells suggest that the deterioration of nuclear selectivity is a consequence of accumulated damage in old NPCs.

## RESULTS

### Life-long stability of *C. elegans* scaffold nucleoporins

As a first approach to characterize how NPCs are maintained in differentiated cells, we decided to analyze if there were differences in the expression of scaffold nucleoporins between dividing and post-mitotic cells. We reasoned that if new pores are assembled in non-dividing cells, scaffold nucleoporins that are essential for NPC assembly into the NE such as the Nup107/160 complex (D'Angelo et al., 2006), should be expressed. In contrast, if pore assembly is restricted to dividing cells, the expression of scaffold nucleoporins could be repressed as soon as cells exit the cell cycle.

To distinguish between these two scenarios we analyzed nucleoporin expression levels during the development of *Caenorhabditis elegans*, a well-characterized nematode from which different developmental stages can be separated manually. Importantly for this study, embryos and larvae contain dividing cells, while somatic cells of adult worms are entirely post-mitotic. We generated stable worm lines expressing GFP under the promoter of a peripheral nucleoporin, ceNup153, or under the promoter of a scaffold nucleoporin, ceNup160. Driven by the ceNup153 promoter, GFP was expressed in most if not all cells of embryos and adult worms (Figure 1B, S1A). In contrast, the ceNup160 promoter-driven expression of GFP was restricted to the embryo and, except for a few neurons in the head (Figure 1C), was not detectable in adult worms (Figure 1B). Strikingly, even in embryos the ceNup160 promoter was only active in a few cells that likely represent dividing cells, as evidenced by the co-expression with cyclin B (Figure S1B, C). It is important to note that the lack of promoter activity for both nucleoporins in the dividing germline is likely due to transgene silencing associated with this technique and not to the lack of promoter activity in the cells. These experiments indicate that expression of the ceNup160 scaffold nucleoporin is tightly regulated during development and absent in post-mitotic cells.

The lack of ceNup160 expression in adult worms raised the question whether the protein was present in the NPCs of adult cells. To test this, we generated stable worm lines expressing full-length ceNup160 or ceNup153 fused to GFP, again under their own promoters, and found that both nucleoporins were present in all embryonic, larval and adult nuclei (Figure 1B). The correct incorporation of the GFP-tagged nucleoporins into *C. elegans* NPCs was confirmed by co-localization with endogenous nucleoporins (Figure 1D).

To directly confirm that Nup160 was not expressed in post-mitotic cells we fed worms that stably expressed ceNup160-GFP or ceNup153-GFP bacteria expressing GFP RNAi for several generations until we obtained transgenic adult worms with no detectable GFP signal. When RNAi-mediated gene knock-down of ceNup160-GFP and ceNup153-GFP was reversed in this adult worms by RNAi against *C. elegans dicer* (*DCR-1*), an essential component of the RNAi machinery (Ketting et al., 2001), only ceNup153-GFP expression was restored (Figure 1E), further supporting the idea that ceNup160 is not expressed in post-mitotic cells. Taken together these results suggest that ceNup160 protein found in adult worms originates from embryonic expression and is extremely stable.

To analyze if other scaffold nucleoporins showed a similar behavior, we obtained worm lines expressing tomato under ceNup133 promoter or ceNup133-tomato under its own promoter. Similar to our findings for ceNup160, the promoter of ceNup133 was restricted to the pharynx cells and a few neurons in the post-mitotic adult worms while the ceNup133 protein was present in every nucleus (Figure S1D). These results indicate that the life-long stability is a common feature of scaffold nucleoporins.

## Expression of scaffold nucleoporins is strongly down regulated during *C. elegans* development

The dramatic difference in the transcriptional regulation of ceNup153 and the scaffolds ceNup160 and ceNup133 components in differentiated cells prompted us to analyze the mRNA levels of other nucleoporins. Since wild type worms contain a large number of dividing cells in their gonads, we used *C. elegans glp-4* mutant animals (strain SS104), which have normal morphology and brood size at 15°C, but lack gonads and are unable to produce germ cells at 25°C (Beanan and Strome, 1992) (Figure 2A). Consistent with this phenotype, adult *glp-4* mutant animals were essentially free of dividing cells as indicated by the absence of cyclin B mRNA (Figure S2A). While the mRNA levels of all tested nucleoporins and lamin were lower in adult worms compared to embryos, only the scaffold nucleoporins, such as ceNup107/160 complex, ceNup205 and ceNup155 were reduced to similar levels than cyclin B (Figure 2B). An exception was the ceNup107/160 complex member ceSec13, which remained highly expressed in adults, consistent with its additional function in COPII-mediated vesicular transport (Salama et al., 1993). Nucleoporin down-regulation was dependent on cell-cycle exit since adult worms containing gonads with dividing cells exhibited high levels of nucleoporin expression (Figure 2A, C). These results suggest that the expression of scaffold nucleoporins, in contrast to peripheral NPC components, is either strongly down-regulated or absent in non-dividing cells.

## Expression of scaffold nucleoporins is not required during adulthood

Despite the low amounts of scaffold nucleoporin mRNAs in post-mitotic cells and the absence of detectable GFP expression from the ceNup160 promoter, it was still possible that low levels of nucleoporin production were sufficient to maintain nuclear integrity in post-mitotic cells. To directly test this we knocked-down nucleoporin mRNAs by RNAi in N2 (wild type) and *daf-2(e1370)* mutant worms, the latter having extended life span due to a mutation in the insulin/IGF-1 receptor (Kenyon et al., 1993; Kimura et al., 1997) and analyzed their life span. The mRNA levels of all tested knockdowns were further reduced by >60–90% (Figure S2B). If low levels of scaffold nucleoporins were required for nuclear function we expected the knockdown to either reduce the life span of adult worms and/or their nucleoporin protein levels. Consistent with their essential role in pore assembly in dividing cells, RNAi against most of the nucleoporins tested were embryonic lethal (Table 1). However, when the RNAi was performed in post-mitotic adult worms, only the knockdown of dynamic nucleoporins significantly reduced adult life span, while none of the scaffold nucleoporins had a measurable effect, even when depleted in long-lived worms (Figure 3A, Figure S2C). Similar to previous

results (Haithcock et al., 2005), knock-down of the single lamin gene was lethal to adult worms with lethality rates comparable to that of ceNup153 (Figure 3A). Notably, the protein levels of the scaffold ceNup107 and ceNup160 nucleoporins in post-mitotic worms remained high during the persistent depletion of the corresponding mRNAs by RNAi (Figure 3B, Figure S2D). In contrast, the protein levels of the dynamic ceNup153 and ceNup35 decreased when their mRNAs were knocked-down. When the RNAi was performed in reproductive worms containing the dividing cells of the germline, the total levels of all nucleoporins tested decreased (Figure 3C) consistent with the fact that new NPCs are constantly being assembled in proliferating cells. Taken together these results suggest that the expression of scaffold nucleoporins is not required in the post-mitotic stage, even in long-lived animals.

From the experiments described above we conclude that (i) pore assembly is tightly regulated at the transcriptional level, (ii) NPC assembly ceases upon cell cycle exit, and (iii) NPCs scaffolds can last the entire life span of a metazoan organism.

## Down-regulation of scaffold nucleoporin expression is conserved in mammals

To test if the transcriptional repression and the life-long stability of the NPC scaffold structure could also be observed in mammalian cells, we first compared mRNA levels of nucleoporins in dividing C2C12 mouse myoblasts and terminally differentiated myotubes (Figure S3A) using Q-PCR. Consistent with our findings in *C. elegans*, all nucleoporins tested were highly expressed in dividing myoblasts. However, only the scaffold nucleoporins were strongly down regulated in post-mitotic myotubes (Figure 4A).

In the C2C12 differentiation system ~30% of the cells do not differentiate into myotubes and remain as quiescent cells that maintain the capability of re-entering the cell cycle when exposed to growth factors-rich media. To investigate if the down-regulation of nucleoporin expression occurs during differentiation or when the cells exit the cell cycle, we separated differentiated myotubes from non-dividing quiescent cells and analyzed the mRNA levels of different nucleoporins in comparison with dividing myoblasts. We observed that the shutdown of scaffold nucleoporin expression also occurred in quiescent cells and that releasing the cells into the cell cycle rapidly reactivated nucleoporin expression (Figure 4B). Supporting the idea that the transcriptional repression occurs upon cell cycle exit, we found that most of the down-regulated nucleoporins contain potential binding sites for E2F transcription factors (data not shown), which are key regulators of cell cycle progression/exit (McClellan and Slack, 2007). To test if the Rb/E2F pathway could indeed control the expression of these proteins, we induced the release of the E2F transcription factors from the retinoblastoma proteins in differentiated myotubes by expressing the viral E1A protein fused to the estrogen receptor (Felsani et al., 2006). We found that upon induction of E1A activity with 4-hydroxy tamoxifen in the post-mitotic cells the expression of scaffold nucleoporins was re-activated (Figure 4C). Our results indicate that the transcriptional down-regulation of nucleoporins is conserved from worms to mammals and supports the idea that, due to the lack of expression of essential scaffold nucleoporins, new pore formation ceases upon cell cycle exit. It is interesting to mention that we did not observe re-activation of ceNup160 expression when we depleted the *C. elegans* homologues of retinoblastoma (lin-35) or the E2F transcription factor (elf-1) in post-mitotic worms by RNAi, indicating that even when the down-regulation of nucleoporins during cell cycle exit is conserved, the mechanism involved may vary between species.

Despite the reduction of core nucleoporin expression, the nucleoporin protein levels and the overall number of NPCs (Figure 4D, E) remained high during differentiation, which can only be explained by life-long stability of these proteins.

### Scaffold nucleoporins are not exchanged once inserted into the NE

One prediction from the life-long stability of scaffold nucleoporins is that these proteins would not be exchanged once they are incorporated into the NE. This hypothesis could not be experimentally tested using fluorescence recovery after photobleaching (FRAP) measurements of GFP-tagged nucleoporins, because the lifetime of nucleoporins exceeded the stability of GFP (we noticed a sharp decline in fluorescence intensity of ceNup160-GFP in adult worms although the protein remained stable, data not shown). As an alternative approach we mixed myoblasts expressing GFP-Nup107, a scaffold nucleoporin (Krull et al., 2004) (Walther et al., 2003), Pom121-GFP, a structural transmembrane nucleoporin (Antonin et al., 2005), or Lamin B1-GFP, a component of the nuclear lamina (D'Angelo and Hetzer, 2006), under a constitutive cytomegalovirus (CMV) promoter with untransfected myoblasts and induced the fusion/differentiation into multinucleated myotubes by lowering the serum concentration. We then followed the incorporation of the GFP-tagged proteins into the non-fluorescent nuclei derived from untransfected cells (Figure 5A). As expected, we observed that Pom121-GFP, GFP-Nup107 and Lamin B1-GFP efficiently incorporated into the NPCs and lamina of dividing cells (Figure S3B). In post-mitotic myotubes, Pom121 equilibrated at pores after ~30 hrs (Figure 5B, C and Movie S1). In striking contrast, we did not detect any incorporation (i.e. replacement of endogenous Nup107) of GFP-Nup107 even after two days of imaging (Figure 5B, C, Movie S2). The lack of incorporation was also observed for all other scaffold nucleoporins tested, including Nup93, Nup43 and Seh-1, while all dynamic nucleoporins analyzed exchanged (Figure S3B). Supporting the fact that scaffold proteins cannot be incorporated at the NE of post-mitotic myotubes, prolonged or high expression of these nucleoporins resulted in its cytoplasmic accumulation and the formation of NE associated aggregates (Figure 5D, Figure S3B). Interestingly, the incorporation of Lamin B1-GFP, which has been shown to have a residence time at the NE comparable to the Nup107/160 complex (Rabut et al., 2004a), was similar to Pom121-GFP (Figure 5B, C and Movie S3), indicating the lamina turns over, albeit slowly.

### The scaffold nucleoporin Nup107 exhibits extreme stability

If scaffold nucleoporins are not exchanged once inserted in the NPC, we should expect these proteins to be present in pot-mitotic cells for long periods of time. To test this, we performed pulse-chase experiments using isotope labeling of proteins in C2C12 cells. For this experiment, dividing myoblasts were incubated with an $S^{35}$-methionine/cysteine mix to allow the radioactively-labeled scaffold nucleoporins be incorporated in newly forming NPCs. Cells were then induced to differentiate and nucleoporins were immunoprecipitated and analyzed at different times after differentiation. Consistent with an extreme stability of the NPC scaffold, we found that Nup107 showed no significant degradation over several weeks. In contrast, dynamic nucleoporins, such as Nup62 and Nup153, and structural proteins like tubulin and lamin A turned over rapidly (Figure 5E). Interestingly, histone H2B also showed high stability in post-mitotic cells (Figure 5E), consistent with its reported half-life of 223 days (Commerford et al., 1982). But, unlike Nup107, histone H2B was exchanged from nucleosomes in post-mitotic nuclei (Figure S4A). The observed extreme stability of scaffold nucleoporins is most likely due to the protective environment where these proteins are located; i.e. embedded in the NE and coated with peripheral nucleoporins, and not due to the intrinsic stability of proteins. This notion is supported by the finding that the entire nonameric Nup107/160 complex is rapidly degraded when one of its components is knocked-down by RNAi in dividing cells (Walther et al., 2003). Additionally, we found that the cytoplasmic Nup107 protein that is not incorporated into NPCs in post-mitotic myotubes is degraded (Figure S4B).

Together with our findings in *C. elegans* these results suggest that the NPC scaffold is built to last the lifetime of a cell and once embedded in the NE its subcomponents are not replaced.

### Defects in the permeability barrier of old NPCs lead to a loss of nuclear integrity

Defects in nuclear organization and function have been reported in many old organisms (Haithcock et al., 2005; Scaffidi and Misteli, 2006). Our findings that pores do not turn over in non-dividing cells raise the question whether NPC function is compromised in old cells. Since a central role of the scaffold nucleoporins is to anchor other NPC components that are responsible for the maintenance of the nuclear permeability barrier (Alber et al., 2007; Frosst et al., 2002; Grandi et al., 1997), we decided to test if the NPCs remain functional as cells age. Potential defects in nuclear membrane integrity and the permeability barrier of NPCs can be directly tested using fluorescent dextrans with defined molecular weights as molecules larger than 60 kDa are excluded from intact nuclei (Lenart and Ellenberg, 2006) (Figure S5A). If the permeability barrier of NPCs is compromised, a 70 kDa dextran would be able to leak into the nucleus, whereas perturbations of the nuclear membrane are required to allow access of a 500 kDa dextran (Galy et al., 2003) (Figure S5A). It is important to note that dextran influx assays are more sensitive than measuring active transport through the NPC, since even a single defective pore can be detected (Lenart et al., 2003). To test for functional alterations in old NPCs, we isolated nuclei from post-mitotic adult worms at different ages and analyzed their nuclear permeability. We found that, while both dextrans were excluded from the nuclei of young worms, influx of the 70 kDa dextran but not 500 kDa dextran was observed in a significant percentage (~ 30%) of the old worm nuclei (Figure 6A), indicating that the NPC function becomes compromised with age.

To analyze if these 'leaky nuclei' could also be observed in mammals and to further determine whether this is a general phenomenon of aging, we isolated nuclei from non-proliferative regions of young (3 month) and old (28 month) rat brains and analyzed their permeability to dextrans. Similar to our observations in *C. elegans*, the ability to exclude 70 kDa dextran, but not 500 kDa, declined with age (Figure 6B). To confirm that the influx of dextran occurs through defective NPCs, we tested the effect of the wheat germ agglutinin (WGA), a lectin that binds to several glycosylated nucleoporins and can efficiently plug nuclear pores (D'Angelo et al., 2006), on the observed dextran influx. By using biotinylated WGA in combination with streptavidin we could block the NPCs to an extent where even the diffusion of 10 kD dextran into the nucleus was impeded (Figure S5B). When the old nuclei were treated with WGA under these conditions we found that the 70 kDa dextran no longer diffused inside the nucleus (Figure S5C), demonstrating that the nuclear leakiness is a consequence of a defective NPC permeability barrier.

Interestingly, we observed that the time of dextran equilibration between cytoplasm and nucleoplasm varied considerably among nuclei suggesting that the percentage of defective pores varied between nuclei (data not shown). This fits well with the idea of a gradual loss of the pore permeability function over time. One consequence from such a progressive deterioration of pore function would be the leaking of cytoplasmic proteins into the nucleus, as happens when NPCs are partially dismantled during mitosis (Lenart et al., 2003). Supporting this idea, we found that the rat nuclei that failed to exclude 70 kDa dextran, exhibited intranuclear tubulin bIII, a strictly cytoplasmic protein (Figure 6C). In many cases nuclear tubulin had aggregated into large filamentous structures that caused severe morphological chromatin aberrations (Figure 6D). These extensive aggregates of a cytoplasmic protein are likely the result of a long-term accumulation process and support the idea that the loss of nuclear integrity occurred over time *in vivo* and not during nuclei isolation. These results further suggest that the observed permeability defects are directly linked to defective pores and not NE perturbations as observed in age-related diseases such as progeria, where mutant lamins perturb the nuclear membrane (Scaffidi and Misteli, 2006). In agreement with this, we found no differences in the nuclear lamina structure, the inner nuclear membrane proteins or the

distribution of NPCs in intact and leaky nuclei, all phenotypes associated with alterations in NE and lamin proteins (Figure S5D, E) (D'Angelo and Hetzer, 2006).

## Age-related deterioration of nuclear pore complex structure and function

Taken together, our results suggest that the long-lived NPC structure deteriorates over time leading to an increase in nuclear permeability with age. To investigate the presence of defects in the nuclear pore complexes from old nuclei we stained leaky and intact nuclei with different antibodies against structural components. Strikingly, we noticed that Nup93, but not Nup107 or Pom121, was lost from the old leaky nuclei (Figure 7A, C, Figure S6A). Since Nup93 has been shown to be critical for establishing the NPC permeability barrier (Galy, 2003), the observed age-related loss of this nucleoporin provides a molecular explanation for the influx of 70 kDa in old nuclei. Interestingly, Nup93 has been shown to interact with FG-nucleoporins from the central channel and it is believed to help establish the NPC diffusion barrier by recruiting these nucleoporins to the pore (Alber et al., 2007; Frosst et al., 2002; Grandi et al., 1997). Supporting this model, we found that the leaky nuclei also showed a decreased staining for mAb414, an antibody that recognizes several FG-nucleoporins such as Nup62 from the central channel (Davis and Blobel, 1987) (Figure 7B, C).

These results raise the question why the scaffold Nup93, but not Nup107, is lost during aging? One possibility is that due to their location in the NPC structure, the Nup107/160 complex is protected from cytosolic agents while Nup93 is exposed to the central channel and might therefore be more accessible to damage that could alter its function. Oxidative protein damage caused by reactive oxygen species (ROS) has been shown to increase during aging and has been linked to a wide range of protein defects (Chakravarti and Chakravarti, 2007; Dalle-Donne et al., 2006). Consistent with this, we found a sharp increase in the levels of protein carbonyl groups, which are indicative of oxidative protein damage, in old versus young nuclei (Figure S7A). Interestingly, when we analyzed if nucleoporins were targets of oxidative damage we found that Nup93 and Nup153, but not Nup107, showed the presence of carbonyl groups (Figure 7D). These findings support the idea that the scaffold Nup107/160 complex, but not Nup93/205, are protected from damage and might explain why it is not lost from NPCs during aging.

If the observed NPC functional defects are indeed caused by ROS, we could expect that inducing oxidative stress in post-mitotic cells would accelerate the appearance of leaky pores. To test this, we treated SS104 adult day 1 worms with N,N′-Dimethyl-4,4′-bipyridinium dichloride (paraquat), a known oxidative stress inducer that significantly increases ROS in worms (Kim and Sun, 2007; Oeda et al., 2001) for 6 days. Strikingly, we found that the worms treated with paraquat showed a higher percentage and earlier onset of leaky nuclei when compared to control worms (Figure 7E). In contrast, when we analyzed nuclei isolated from SS104 worms grown for 8 days on empty vector (control) or daf-2 RNAi, which increases life span and the tolerance to oxidative stress (Honda and Honda, 1999; Kim and Sun, 2007), we found the reciprocal effect with the long-lived worms having a lower percentage of leaky nuclei than the control worms (Figure 7F).

To further confirm that the age-dependent increase in nuclear permeability occurs *in vivo* and is accelerated by oxidative stress, we injected worms of different days of adulthood with a 70 kDa dextran and analyzed its diffusion into the nucleus. Lamin-GFP served as a marker to identify the NE. Consistent with our data from isolated nuclei, we detected that old worms had an increased nuclear permeability compared to young worms and that nuclear leakiness was strongly increased by the treatment with paraquat (Figure S7B). Together these results suggest that oxidative protein damage can cause the deterioration of the pore permeability barrier and indicates that the appearance of pore defects is directly linked to the aging process. This may

explain why the loss of nuclear selectivity occurs at different time scales in different organisms (i.e. days in worms versus months in rats).

## DISCUSSION

The results presented in this work indicate that the biogenesis of nuclear pore complexes is restricted to mitotic stages and ceases upon cell cycle exit. We demonstrate that NPC scaffold members do not turn over and show life-long residence at the NPC in non-dividing cells. The finding that nuclear pore structure and function deteriorates with age suggests that the presence of the same nucleoporins during the entire life span of post-mitotic cells comes at the physiological cost of aging-related pore defects that lead to a loss of nuclear integrity.

Why would cells keep the same NPC scaffolds during their entire life? Two reasons to explain this can be imagined: 1) if new pores were to be inserted into the NE of post-mitotic cells, then old pores would have to disassemble in order to maintain NPC number. As NPC disassembly is accompanied by an increase in nuclear permeability, non-dividing cells would have to employ a disassembly mechanism that prevents a continuous loss of the nuclear permeability barrier. No evidence of such a mechanism has been found so far. 2) If no new pores were to be inserted in the NE but the subunits of pre-existing scaffolds were able be replaced with newly synthesized ones, then cells would have to replace the components of the eight-fold symmetrical scaffold one by one in order to maintain the nuclear permeability barrier. Considering that the cores are embedded in the NE and covered by multiple layers of peripheral nucleoporins, it is difficult to imagine a molecular mechanism that would ensure such coordination and specificity based on the current knowledge of the pore. Therefore NPC turnover appears to be restricted to mitosis, where an orchestrated program of phosphorylation events leads to the rapid disassembly of the entire pore complex (Burke and Ellenberg, 2002).

Our findings indicate that in organisms that divide by closed mitosis (i.e. they divide without NE breakdown), such as *Saccharomyces cerevisiae*, the NPC scaffold should remain embedded in the NE for many generations. Consistent with this idea, it was recently shown that NPCs stay associated with the mother cell in a process that is mediated by the asymmetric segregation of NPCs during yeast mitosis (Shcheprova et al., 2008). It is therefore tempting to speculate that mother cells, which are already known to retain damaged proteins (Aguilaniu et al., 2003), also accumulate defective NPCs that might contribute to their overall aging process.

The lack of a replacement mechanism for scaffold nucleoporins in non-dividing cells indicates that some differentiated cells, such as muscle fibers and neurons, would keep the NPC scaffolds for many years. These long-lived nucleoporins might therefore be particularly vulnerable to protein damage as cells age. Consistent with this idea, we found that Nup93, but not the Nup107 protein, can suffer from oxidative damage in old cells. As stated above, these differences may be a consequence of their location inside the NPC structure. While the Nup107/160 complex is embedded in the nuclear membrane and shielded by several layers of proteins, the Nup93 complex, which acts as a linker between the Nup107/160 scaffold and the FG-nucleoporins from the central channel (Alber et al., 2007), is exposed to the cytoplasmic factors that can access the pore channel. Thus, Nup93, which like Nup107 is not replaced in non-dividing cells, might accumulate damage over time to a point where it can no longer remain bound to the NPC. The absence of the Nup93 protein linker would result in a loss of FG-nucleoporins and a deterioration of the permeability barrier. This provides a molecular explanation for the phenomenon of old leaky nuclei we observed, which potentially represents an early event in the previously described deterioration of old nuclei (Haithcock et al., 2005).

Interestingly, we discovered that one third of the nuclei purified form old differentiated cells show defects in the nuclear permeability barrier and the accumulation of cytoplasmic tubulin bIII, a finding consistent with a loss of nucleo-cytoplasmic compartmentalization. Strikingly, tubulin-positive intranuclear filaments have been described in many mammals, including humans, and their occurrence has been linked to the aging process as well as to neurodegenerative diseases such as Alzheimer and Parkinson (Woulfe, 2007), all of which have been associated with elevated oxidative damage (Danielson and Andersen, 2008; Zhu et al., 2007). This raises the intriguing possibility that defective pores may be associated with all of these diseases. It will be interesting to investigate the molecular deterioration of NPCs in a time resolved manner and to study in detail how the loss of nuclear integrity due to defective pores contributes to cellular aging and to the onset of age-related diseases.

## EXPERIMENTAL PROCEDURES

### Antibodies

Anti-ceNup35 (NPP-19), anti-ceNup107 (NPP -5) and anti-ceNup153 (NPP -7) were kindly provided by P. Askjaer (Galy et al., 2003). Anti-Ndc1 and anti-Nup153 antibodies were a gift of U. Kutay (Mansfeld et al., 2006) and B. Burke (Bodoor et al., 1999). Anti-Nup107 used for immunofluorescence studies was a gift of V. Doye (Belgareh et al., 2001). Anti-Lap2b was a gift from R. Foisner. Anti-Myosin Heavy Chain antibody (MF-20), anti-GAPDH (6C5) and anti-H2B were purchased from Developmental Studies Hybridoma bank at the University of Iowa, Abcam and Upstate respectively. Anti-tubulin (B512) and anti-Lamin A (L1293) were purchased from Sigma. Anti-tubulin bIII and mAb414 were from Covance. Anti-Nup93 (3332 C2a) was purchase from Santa Cruz. Anti-ceNup160 (NPP -6) and mammalian Nup43, Sec13 and Nup107, used for western blot and immunoprecipitation studies, were generated by injecting rabbits with GST-ceNup160 (aa1183–1586), His-hSec13, MBP-hNup43, and His-mNup107 (aa600–926) recombinant proteins. Antibodies against Nup107 and Nup93 were generated against the first 150 amino acids of the corresponding human protein.

### Cells

C2C12 cells were obtained from ATCC and grown at 37°C in a 5% CO2 containing incubator. Proliferating myoblast were maintained in DMEM + 20% fetal bovine serum. Differentiation into myotubes was induced at 90% confluence by shifting to DMEM + 2% horse serum. Fresh media was added every 2–3 days. Myotubes were separated from quiescent cells on day 6 of differentiation with 0.025% trypsin. Transfection of myoblast cells was performed at low density using Optifect (Invitrogen).

### Worm strains

Worms were grown at 15°C and maintained as described (Brenner, 1974). The strains used in this study were obtained from the *Caenorhabditis* Genetics Center CGC, Minneapolis, MN and include the following: N2 wild-type, *daf-2(e1370)* mutant and the temperature sensitive sterile CF512 *fer-15(b26)II; fem-1(hc17)IV* and SS104 *glp-4(bn2)I* mutants. The Cyclin B-YFP strain [Pcyb-1::cyb-1::yfp] was kindly provided by M. Hengartner. The YG065 Lamin-GFP strain [Pbaf-1::lmn-1::gfp] was a gift of Y. Gruenbaum.

### Synchronization of temperature sensitive sterile animals

Age-synchronized worms were obtained at 25°C using the CF512 or SS104 temperature-sensitive sterile strains as described (Raices et al., 2005). Synchronized larvae or adult worms were harvested at different time points and nucleoporin expression was analyzed by semi-quantitative RT-PCR, Q-PCR or western blotting.

### RNAi inhibition using *DCR-1*

ceNup160-GFP and ceNup153-GFP expressing worms were grown on *GFP* dsRNA for several generations until no GFP signal was detected. To lower the *GFP* RNAi activity animals were shifted to bacteria expressing *DCR-1* dsRNA (Dillin et al., 2002) as day 1 adults. Control animals were grown on bacteria containing the empty vector and shifted to *DCR -1* RNAi bacteria at the same time (data not shown). Worms were grown for 6 days on *DCR -1* RNAi before imaged.

### Generation of *C. elegans* transgenic lines

*C. elegans* transgenic worms were generated using the N2 wild type strain as previously described (Panowski et al., 2007). For vectors expressing GFP under ceNup160 or ceNup153 endogenous promoter, a 4 kilobase sequence upstream of the corresponding coding region was amplified from genomic DNA and cloned upstream of GFP in the pPD95.77. Vectors expressing GFP-tagged full-length ceNup160 and ceNup153 were generated by subcloning genomic *ceNup160* or *ceNup153* in frame and upstream of the GFP sequence in the vectors described above. The ceNup133 promoter and full-length reporters were generated by cloning the 429 bp region upstream of the start codon (promoter) or this region plus the full *ceNup133* gene (full length) in a pPD95.77 vector where GFP had been replaced by the tomato gene. For each construct at least 3–5 worm lines were analyze.

### RNAi

HT115 bacteria expressing dsRNA were grown at 37°C in LB with 10 mg/ml tetracycline and 50 mg/ml carbenicillin, then seeded onto NG-carbenicillin plates and supplemented with 0.1M IPTG (1.5 mM final concentration). Adult worms were added to plates and animals were transferred to new plates every 2–3 days. RNAi clones used in this study are summarized in Table S1. Julie Ahringer's and Marc Vidal's library clones were a gift of A. Dillin (Salk, La Jolla, USA). pAD12 (Bluescript vector with opposing T7 promoters) was used as empty vector control. Nup93 RNAi vector was kindly provided by P. Askjaer.

For embryonic lethality assays, the total number of progeny born to a single worm over time was measured in the following way. Worms hatched within a 1 h period were collected and allowed to develop to the L4 stage. Once in the L4 stage, worms were individually placed onto separate RNAi plates. In all cases, at least 15 worms were used for each analysis. Worms were transferred to new plates every 12 hours and the resulting progeny were allowed to grow for two days until counted for progeny measurements. The % of total progeny was calculated by dividing the number of progeny produced on each RNAi treatment by the total number of progeny produced by the vector control treatment. To determine the effect of RNAi on nucleoporin protein level in synchronized adult worms, a minimum of 5000 SS104 worms were grown at 25°C (restrictive temperature) in the corresponding dsRNA expressing bacteria and collected at the indicated time points. In parallel, synchronized worms were grown at 15° C on the same dsRNA bacteria plates to produce a reproductive population of worms that was used as mitotic control. Protein was prepared as described below.

For nuclei permeability assays, a minimum of 60,000 worms adult SS104 worms were transferred in day 1 of adulthood to plates containing control bacteria (carrying the pAD12 vector), or bacteria expressing daf-2 RNAi. Worms were transferred to fresh plates every 2 days. After 6 days, nuclei were isolated and used for nuclear permeability assayed (see below).

### Survival Analysis

Life span assays were performed at 20°C and RNAi treatments were initiated at day 1 of adulthood. Animals (100–130 per experiment) were transferred away from their progeny to

new plates every day until the end of the reproductive period. JMP software was used to carry out statistical analysis and to determine mean life spans and 75th percentiles. The logrank (Mantel-Cox) statistics was used to evaluate the hypothesis that animals in experimental and control groups behaved similarly. Animals that crawled off the plate, "exploded" (i.e., had a gonad extruding through their vulva), or "bagged" (i.e., died from internal hatching) were censored at the time of the event and were incorporated into the data set as described (Ketting et al., 2001). RNAi efficiency was controlled by determining embryonic lethality and by Q-PCR.

### RNA isolation, semi-quantitative RT–PCR and quantitative Q-PCR

*C. elegans* total RNA was isolated from embryos and synchronized populations of larvae and adult worms using TRIzol reagent (Invitrogen). C2C12 total RNA was prepared from proliferating myoblasts, quiescent myoblasts or differentiated myotubes using Qiagen RNeasy kit. cDNA was created using 3 μg of total RNA, oligo dT primers and SuperScript™ III Reverse Transcriptase (Invitrogen). For semi-quantitative RT PCR, serial dilutions of 5, 10, 20 and 40 were used for PCR reactions. mRNA specific primers were designed on exon junctions (Table S2) and their inability to amplify genomic DNA was tested. For each primer pair, cycle times and primer concentrations were optimized to ensure linear amplification. Quantification was performed on 20 dilution reactions using ImageQuant™(GE healthcare) software and levels were normalized to *C. elegans* actin (*ACT-1*) mRNA levels.

*C. elegans* SybrGreen real-time Q-PCR experiments were performed as described in the manual using ABI 7900HT (Applied Biosystems) and cDNA at a 1:20 dilution. mRNA levels were normalized to actin (*ACT-1*). C2C12 Q-PCR analyses were performed as described (Bookout et al., 2006). GAPDH mRNA levels were used to normalized mammalian nucleoporin expression. All primers used can be found in Table S2.

### Expression of viral E1A in differentiated myotubes

Retrovirus carrying the control estrogen receptor (ER) or the E1A fused to the ER were generated in Phoenix cells and used to infect C2C12 myoblasts. Infected cells were selected in puromycin containing media for 48–72 hs and induced to differentiate for 3 days. E1A activity in differentiated myotubes was induced with 1mM 4OH-tamoxifen (Sigma) for 24 hs. Cells were then collected and total RNA was extracted. Nucleoporin expression levels were analyzed as described before. The retroviral vectors used in this study were a gift of Clodagh O'Shea.

### Protein extracts and western blot analysis

*C. elegans* protein extracts were prepared by mixing 1 volume of worms with 1 volume of glass beads (100–300 mM) and 2 volumes of 2X SDS buffer (240 mM Tris-HCl at pH 6.8, 4% SDS, 16% glycerol + protease inhibitors) preheated to 95°C using a vortex. The mixed samples were incubated at 95°C for 5 minutes. This was followed by two cycles of 1 minute vortex and 2 minutes 95°C. For C2C12 total protein extracts, proliferating myoblasts or differentiated myotubes were scrapped from plates using 1X SDS buffer preheated to 95°C, incubated at 95° C for 5 minutes and passed 5–10 times though a 27 gauge syringe. Protein concentration was determined using the BCA reagent (Pierce), normalized and b-mercaptoethanol + bromophenol blue were added to a final concentration of 4% and 0.01% respectively.

For western blot analysis 40–80 mg of total protein extracts were resolved in SDS-polyacrilamide gels and transfer to Immobilon-FL membranes (Millipore). Blotted membranes were blocked with PBS-T (Phosphate buffer saline containing 0.05% Tween 20) containing 5% non-fat milk for 1 h, washed once with PBS-T and incubated with the corresponding primary antibody for 1 h at room temperature or over-night at 4°C. Excess of antibody was

removed by washing 3 times with PBS-T and the secondary antibody was added for 1 h at room temperature. After 3 washes with PBS-T membranes were analyzed and quantified using an Odyssey infrared imaging system from LI-COR Biosciences. *C. elegans* protein levels were normalized to a-tubulin while C2C12 protein levels were normalized to glyceraldehyde 3-phosphate dehydrogenase (GAPDH).

### Pulse chase experiments

C2C12 myoblasts at ~50% confluency were incubated in pulse media (DMEM lacking methionine and cysteine plus 15% dialyzed FBS) containing 100 mCi/ml of mixture of $S^{35}$-methionine and $S^{35}$-cysteine for 24 hs (EasyTag™ EXPRESS35S Protein Labeling Mix, Perkin Elmer). The pulse media was then replaced by DMEM + 20% FBS for 12 hs and the confluent cells were switch to differentiating media (DMEM + 2% horse serum). Samples were collected at the indicated time points and froze in liquid N2 until processed. Total protein extracts were prepared by lysing the cells in hot 50 mM Tris pH8, 0.5% SDS and 1 mM DTT using a 27G syringe. Extracts were corrected with 4 volumes of RIPA correction buffer (50 mM Tris pH8, 187 mM NaCl, 1.25% NP-40, 1.25% DOC) and immunoprecipitated (IP) with specified antibodies. IP proteins were resolved by SDS-PAGE, transferred to PVDF membranes and analyzed by western blotting. The same membranes were later dried and exposed autoradiography film to revealed the $S^{35}$ signal.

### Isolation of *C. elegans* and rat nuclei and analysis of nuclear permeability

For *C. elegans* nuclei purification, worms at different days of adulthood were frozen in 1 volume of PBS buffer, thawed in ice and transferred to a pre-chilled Wheaton stainless-steel tissue grinder (clearance 0.0005 inches/12.5 μm). An equal volume of 2X Nuclear Preparation Buffer (NPB) containing 20 mM Hepes pH7.6, 20 mM KCl, 3 mM MgCl2, 2 mM EGTA, 0.5 M sucrose, 1 mM PMSF and 1X Complete Protease Inhibitor Cocktail (Roche) was added. Homogenization was performed with 3–4 sets of one stroke. To ensure complete homogenization and that nuclei were intact, a small aliquot of the preparation was visualized under a bright field microscope and under a fluorescent microscope by adding DAPI to 1 μg/ml. Nuclei were concentrated by centrifugation at 800 Xg for 10 minutes, washed with 2X NPB buffer and resuspended in S500 buffer (20 mM Hepes pH 7.4, 50 mM KCl, 1 mM MgCl2, 0.5 M sucrose) containing protease inhibitors.

For the preparation of rat nuclei, the brain cortex of young (3 months) and old (28 months) Fischer 344 female rats were dissected and carefully minced. Nuclei were isolated as described by Lovtrup-Rein and McEwen (Lovtrup-Rein and McEwen, 1966). To analyze if there were differences in the nuclear permeability barrier of young versus old nuclei, the isolated *C. elegans* and rat nuclei were incubated with a mixture of FITC-70 kDa and TRITC-500kDa dextrans (Sigma) plus hoechst for 15–30 minutes. Influx of dextrans inside the nuclei was analyzed in unfixed samples by confocal microscopy. The percentage of nuclei with alter permeability barrier was quantified using Adobe Photoshop CS3 Extended.

In parallel rat nuclei were incubated with the FITC-70 kDA dextran alone, fixed with 4% paraformaldehide (PFA) and immunostained with an anti-Tubulin bIII antibody.

### Oxidative stress treatment and analysis

The analyses of proteins carbonylation were performed using the Oxyblott™ Protein Detection Kit from Millipore. For immunofluorescence studies isolated young and old rat nuclei were fixed with PFA 4% and spun down onto polylysine treated coverslips. The nuclei were washed with PBS and treated with 2,4-dinitrophenylhydrazine to derivatize carbonyl groups to 2.4-dinitrophenylhydrazone (DNP-hydrazone) The DNP-derivatized proteins were detected by immunofluorescence using undiluted anti-DNP antibody. To determine the presence of

carbonyl groups in the Nup93, Nup153 and Nup107 nucleoporins, total protein extracts from brains of old rats (28 months) were prepared by homogenizing in hot 50 mM Tris pH8, 0.5% SDS and 1 mM DTT using a 27G syringe. Extracts were corrected with 4 volumes of RIPA correction buffer (50 mM Tris pH8, 187 mM NaCL, 1.25% NP-40, 1.25% DOC) and immunoprecipitated (IP) with specified antibodies. Carbonyl groups in proteins were treated with 2,4-dinitrophenylhydrazine as described above. Derivatized proteins were resolved by SDS-PAGE, transferred to PVDF membranes and analyzed by western blotting using an anti-DNP antibody to determine the presence of carbonyl groups and the specific nucleoporin antibodies to determine protein levels.

To analyze the effect of oxidative stress on the nuclear permeability of post-mitotic worms, SS104 adult day 1 animals were transferred to plates containing bacteria or bacteria plus paraquat (0.5mM final). Worms were transferred to fresh plates on day 3 and collected on day 6 to isolate nuclei and perform nuclear permeability assays as described. For studies of nuclear permeability *in vivo*, adult worms were grown for 6 days in the presence of 1mM paraquat before injected as described below.

### Injection of dextran in adult worms

Adult worms expressing Lamin-GFP were injected in the intestine at the specified days of adulthood with a TRITC-70 kDa dextran. After 20 minutes worms were the dextran had entered intestinal cells were separated and analyzed for nuclear permeability by confocal microscopy ($n \geq 10$).

### Microscopy

Transgenic worms were grown on OP50 *E. coli* and images were taken on different developmental stages. GFP expression was analyzed with a Leica 6000B digital microscope and images were acquired using Leica FW4000 software. GFP is shown in green and is merged with differential interference contrast images. The correct localization of *C. elegans* nucleoporin in transgenic worms was analyzed using an SP2 confocal microscope (Leica). When comparing fluorescence intensity, non-saturated maximal projections of 30–40 confocal sections were obtained using the SP2 confocal microscope. Images were processed using Imaris software by Bitplane. Black and white images represent only the GFP channel with fluorescence shown in white.

For NPC incorporation analysis of Nup160-GFP and Nup153-GFP fusions in transgenic worms were prepared as described, fixed with 4% PFA and stained with mAb414. NPC localization was analyzed by confocal microscopy.

Nuclear volume and NPC density was used to estimate NPC number during differentiation. C2C12 proliferating myoblasts were transfected with a 3GFP-NLS expressing vector and induce to differentiate. At different time points cells were fixed with 4% PFA and NPCs were stained with anti-Nup153 antibody. Cells were analyzed by confocal fluorescence and nuclear volume was determined form 3D reconstructions (~50 confocal sections) of nuclei that had imported fluorescently labeled 3GFP-NLS. NPC density was determined by counting the number of pores/$mm^2$. Images were processed using Imaris software by Bitplane.

To investigate the incorporation of GFP-tagged Nup107, Nup93, Nup43, Seh1, Pom121, Gp210, Nup50 or Lamin B1 into the NE of differentiated myotubes, C2C12 myoblast cells were transfected with the corresponding constructs, diluted with untransfected cells, grew to confluency and induced to differentiate for 3 days on m-slide 8 well tissue culture treated chambers (Ibidi). Live cells were imaged at 37°C maintained by air stream incubator and enriched with $CO_2$ (Solent Scientific). Time-lapse images of 9 z-stacks were taken every hour

with a 63X oil objective on a custom built spinning disk confocal microscope (McBain Instruments). Images were captured on an EM-CCD digital camera (Hamamatsu) and acquired using SimplePCI (Compix). Maximal projections of the Z-stacks were assembled in SimplePCI and avi files were exported. Avi files were then separated into tiffs and processed in Adobe Photoshop CS3 Extended to generate the figures. The pEGFP vectors expressing the GFP-nucleoporins were a gift of J. Ellenberg (Rabut et al., 2004a) and Lamin B1-GFP was a gift of E. Schirmer.

To analyze the exchange of histone H2B from nucleosomes, proliferating myoblasts were co-transfected with H2B-Tomato and GFP-Nup107 expressing vectors. Cells were induced to differentiate for 3–5 days and myotubes were imaged unfixed by confocal microscopy.

For immunofluorescence studies in isolated rat nuclei, samples were fixed in PFA 4%, spun down onto polylysine coated coverslips and immunostained with the specified antibodies. Note that when analyzing Nup93 short fixation times (1 min) were required for detection.

## Supplementary Material

Refer to Web version on PubMed Central for supplementary material.

## Acknowledgments

We thank P. Askjaer, B. Burke, J. Ellenberg, R. Foisner, M. Hengartner Y. Gruenbaum, U. Kutay, C. O'Shea and E. Schirmer for antibodies, expression vectors and worm strains, M. Downes for the mammalian Q-PCR assays, J. Jepsen for the isolation of rat brains, A. Dillin for reagents and useful comments, the Hetzer lab, C. Hetzer-Egger, T. Hunter, W. Eckhart, F. Gage, and S. Pfaff for critical discussion and reading of the manuscript.

## References

Aguilaniu H, Gustafsson L, Rigoulet M, Nystrom T. Asymmetric inheritance of oxidatively damaged proteins during cytokinesis. Science 2003;299:1751–1753. [PubMed: 12610228]

Alber F, Dokudovskaya S, Veenhoff LM, Zhang W, Kipper J, Devos D, Suprapto A, Karni-Schmidt O, Williams R, Chait BT, et al. The molecular architecture of the nuclear pore complex. Nature 2007;450:695–701. [PubMed: 18046406]

Antonin W, Franz C, Haselmann U, Antony C, Mattaj IW. The Integral Membrane Nucleoporin pom121 Functionally Links Nuclear Pore Complex Assembly and Nuclear Envelope Formation. Mol Cell 2005;17:83–92. [PubMed: 15629719]

Apfeld J, Kenyon C. Cell nonautonomy of C. elegans daf-2 function in the regulation of diapause and life span. Cell 1998;95:199–210. [PubMed: 9790527]

Beanan MJ, Strome S. Characterization of a germ-line proliferation mutation in C. elegans. Development 1992;116:755–766. [PubMed: 1289064]

Beck M, Forster F, Ecke M, Plitzko JM, Melchior F, Gerisch G, Baumeister W, Medalia O. Nuclear pore complex structure and dynamics revealed by cryoelectron tomography. Science 2004;306:1387–1390. [PubMed: 15514115]

Belgareh N, Rabut G, Bai SW, van Overbeek M, Beaudouin J, Daigle N, Zatsepina OV, Pasteau F, Labas V, Fromont-Racine M, et al. An evolutionarily conserved NPC subcomplex, which redistributes in part to kinetochores in mammalian cells. J Cell Biol 2001;154:1147–1160. [PubMed: 11564755]

Bodoor K, Shaikh S, Salina D, Raharjo WH, Bastos R, Lohka M, Burke B. Sequential recruitment of NPC proteins to the nuclear periphery at the end of mitosis. J Cell Sci 1999;112 ( Pt 13):2253–2264. [PubMed: 10362555]

Bookout AL, Jeong Y, Downes M, Yu RT, Evans RM, Mangelsdorf DJ. Anatomical profiling of nuclear receptor expression reveals a hierarchical transcriptional network. Cell 2006;126:789–799. [PubMed: 16923397]

Brenner S. The genetics of Caenorhabditis elegans. Genetics 1974;77:71–94. [PubMed: 4366476]

Burke B, Ellenberg J. Remodelling the walls of the nucleus. Nat Rev Mol Cell Biol 2002;3:487–497. [PubMed: 12094215]

Chakravarti B, Chakravarti DN. Oxidative modification of proteins: age-related changes. Gerontology 2007;53:128–139. [PubMed: 17164550]

Commerford SL, Carsten AL, Cronkite EP. Histone turnover within nonproliferating cells. Proc Natl Acad Sci U S A 1982;79:1163–1165. [PubMed: 6951165]

Crittenden SL, Leonhard KA, Byrd DT, Kimble J. Cellular analyses of the mitotic region in the Caenorhabditis elegans adult germ line. Mol Biol Cell 2006;17:3051–3061. [PubMed: 16672375]

D'Angelo MA, Anderson DJ, Richard E, Hetzer MW. Nuclear pores form de novo from both sides of the nuclear envelope. Science 2006;312:440–443. [PubMed: 16627745]

D'Angelo MA, Hetzer MW. The role of the nuclear envelope in cellular organization. Cell Mol Life Sci 2006;63:316–332. [PubMed: 16389459]

Daigle N, Beaudouin J, Hartnell L, Imreh G, Hallberg E, Lippincott-Schwartz J, Ellenberg J. Nuclear pore complexes form immobile networks and have a very low turnover in live mammalian cells. J Cell Biol 2001;154:71–84. [PubMed: 11448991]

Dalle-Donne I, Aldini G, Carini M, Colombo R, Rossi R, Milzani A. Protein carbonylation, cellular dysfunction, and disease progression. J Cell Mol Med 2006;10:389–406. [PubMed: 16796807]

Danielson SR, Andersen JK. Oxidative and nitrative protein modifications in Parkinson's disease. Free Radic Biol Med 2008;44:1787–1794. [PubMed: 18395015]

Davis LI, Blobel G. Nuclear pore complex contains a family of glycoproteins that includes p62: glycosylation through a previously unidentified cellular pathway. Proc Natl Acad Sci U S A 1987;84:7552–7556. [PubMed: 3313397]

Dillin A, Crawford DK, Kenyon C. Timing requirements for insulin/IGF-1 signaling in C. elegans. Science 2002;298:830–834. [PubMed: 12399591]

Felsani A, Mileo AM, Paggi MG. Retinoblastoma family proteins as key targets of the small DNA virus oncoproteins. Oncogene 2006;25:5277–5285. [PubMed: 16936748]

Frosst P, Guan T, Subauste C, Hahn K, Gerace L. Tpr is localized within the nuclear basket of the pore complex and has a role in nuclear protein export. J Cell Biol 2002;156:617–630. [PubMed: 11839768]

Galy V, Mattaj IW, Askjaer P. Caenorhabditis elegans nucleoporins Nup93 and Nup205 determine the limit of nuclear pore complex size exclusion in vivo. Mol Biol Cell 2003;14:5104–5115. [PubMed: 12937276]

Grandi P, Dang T, Pane N, Shevchenko A, Mann M, Forbes D, Hurt E. Nup93, a vertebrate homologue of yeast Nic96p, forms a complex with a novel 205-kDa protein and is required for correct nuclear pore assembly. Mol Biol Cell 1997;8:2017–2038. [PubMed: 9348540]

Haithcock E, Dayani Y, Neufeld E, Zahand AJ, Feinstein N, Mattout A, Gruenbaum Y, Liu J. Age-related changes of nuclear architecture in Caenorhabditis elegans. Proc Natl Acad Sci U S A 2005;102:16690–16695. [PubMed: 16269543]

Harel A, Orjalo AV, Vincent T, Lachish-Zalait A, Vasu S, Shah S, Zimmerman E, Elbaum M, Forbes DJ. Removal of a single pore subcomplex results in vertebrate nuclei devoid of nuclear pores. Mol Cell 2003;11:853–864. [PubMed: 12718872]

Honda Y, Honda S. The daf-2 gene network for longevity regulates oxidative stress resistance and Mn-superoxide dismutase gene expression in Caenorhabditis elegans. FASEB J 1999;13:1385–1393. [PubMed: 10428762]

Kenyon C, Chang J, Gensch E, Rudner A, Tabtiang R. A C. elegans mutant that lives twice as long as wild type. Nature 1993;366:461–464. [PubMed: 8247153]

Ketting RF, Fischer SE, Bernstein E, Sijen T, Hannon GJ, Plasterk RH. Dicer functions in RNA interference and in synthesis of small RNA involved in developmental timing in C. elegans. Genes Dev 2001;15:2654–2659. [PubMed: 11641272]

Kim Y, Sun H. Functional genomic approach to identify novel genes involved in the regulation of oxidative stress resistance and animal lifespan. Aging Cell 2007;6:489–503. [PubMed: 17608836]

Kimura KD, Tissenbaum HA, Liu Y, Ruvkun G. daf-2, an insulin receptor-like gene that regulates longevity and diapause in Caenorhabditis elegans. Science 1997;277:942–946. [PubMed: 9252323]

Kiseleva E, Allen TD, Rutherford S, Bucci M, Wente SR, Goldberg MW. Yeast nuclear pore complexes have a cytoplasmic ring and internal filaments. J Struct Biol 2004;145:272–288. [PubMed: 14960378]

Krull S, Thyberg J, Bjorkroth B, Rackwitz HR, Cordes VC. Nucleoporins as components of the nuclear pore complex core structure and tpr as the architectural element of the nuclear basket. Mol Biol Cell 2004;15:4261–4277. [PubMed: 15229283]

Lenart P, Ellenberg J. Monitoring the permeability of the nuclear envelope during the cell cycle. Methods 2006;38:17–24. [PubMed: 16343937]

Lenart P, Rabut G, Daigle N, Hand AR, Terasaki M, Ellenberg J. Nuclear envelope breakdown in starfish oocytes proceeds by partial NPC disassembly followed by a rapidly spreading fenestration of nuclear membranes. J Cell Biol 2003;160:1055–1068. [PubMed: 12654902]

Lovtrup-Rein H, McEwen BS. Isolation and fractionation of rat brain nuclei. J Cell Biol 1966;30:405–415. [PubMed: 5968977]

Mansfeld J, Guttinger S, Hawryluk-Gara LA, Pante N, Mall M, Galy V, Haselmann U, Muhlhausser P, Wozniak RW, Mattaj IW, et al. The conserved transmembrane nucleoporin NDC1 is required for nuclear pore complex assembly in vertebrate cells. Mol Cell 2006;22:93–103. [PubMed: 16600873]

Maul GG, Maul HM, Scogna JE, Lieberman MW, Stein GS, Hsu BY, Borun TW. Time sequence of nuclear pore formation in phytohemagglutinin-stimulated lymphocytes and in HeLa cells during the cell cycle. J Cell Biol 1972;55:433–447. [PubMed: 5076782]

McClellan KA, Slack RS. Specific in vivo roles for E2Fs in differentiation and development. Cell Cycle 2007;6:2917–2927. [PubMed: 17993781]

Oeda T, Shimohama S, Kitagawa N, Kohno R, Imura T, Shibasaki H, Ishii N. Oxidative stress causes abnormal accumulation of familial amyotrophic lateral sclerosis-related mutant SOD1 in transgenic Caenorhabditis elegans. Hum Mol Genet 2001;10:2013–2023. [PubMed: 11590119]

Panowski SH, Wolff S, Aguilaniu H, Durieux J, Dillin A. PHA-4/Foxa mediates diet-restriction-induced longevity of C. elegans. Nature 2007;447:550–555. [PubMed: 17476212]

Rabut G, Doye V, Ellenberg J. Mapping the dynamic organization of the nuclear pore complex inside single living cells. Nat Cell Biol 2004a;6:1114–1121. [PubMed: 15502822]

Rabut G, Lenart P, Ellenberg J. Dynamics of nuclear pore complex organization through the cell cycle. Curr Opin Cell Biol 2004b;16:314–321. [PubMed: 15145357]

Raices M, Maruyama H, Dillin A, Karlseder J. Uncoupling of longevity and telomere length in C. elegans. PLoS Genet 2005;1:e30. [PubMed: 16151516]

Reichelt R, Holzenburg A, Buhle EL Jr, Jarnik M, Engel A, Aebi U. Correlation between structure and mass distribution of the nuclear pore complex and of distinct pore complex components. J Cell Biol 1990;110:883–894. [PubMed: 2324201]

Salama NR, Yeung T, Schekman RW. The Sec13p complex and reconstitution of vesicle budding from the ER with purified cytosolic proteins. Embo J 1993;12:4073–4082. [PubMed: 8223424]

Scaffidi P, Misteli T. Lamin A-dependent nuclear defects in human aging. Science 2006;312:1059–1063. [PubMed: 16645051]

Shcheprova Z, Baldi S, Frei SB, Gonnet G, Barral Y. A mechanism for asymmetric segregation of age during yeast budding. Nature 2008;454:728–734. [PubMed: 18660802]

Walther TC, Alves A, Pickersgill H, Loiodice I, Hetzer M, Galy V, Hulsmann BB, Kocher T, Wilm M, Allen T, et al. The conserved Nup107–160 complex is critical for nuclear pore complex assembly. Cell 2003;113:195–206. [PubMed: 12705868]

Weis K. Regulating access to the genome: nucleocytoplasmic transport throughout the cell cycle. Cell 2003;112:441–451. [PubMed: 12600309]

Woulfe JM. Abnormalities of the nucleus and nuclear inclusions in neurodegenerative disease: a work in progress. Neuropathol Appl Neurobiol 2007;33:2–42. [PubMed: 17239006]

Zhu X, Su B, Wang X, Smith MA, Perry G. Causes of oxidative stress in Alzheimer disease. Cell Mol Life Sci 2007;64:2202–2210. [PubMed: 17605000]

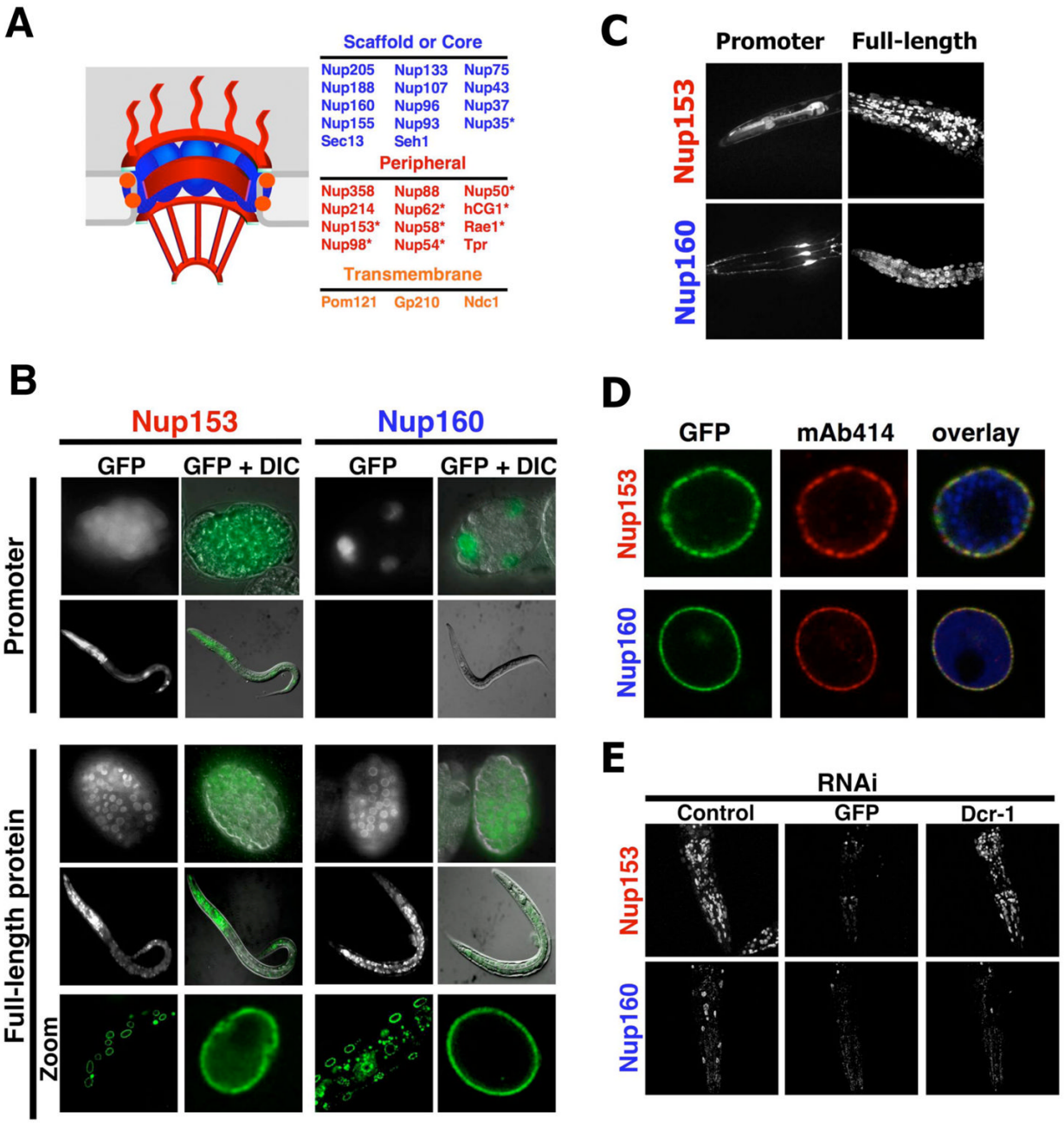


**Figure 1. ceNup160 scaffold nucleoporin shows life-long stability**

**(A)**. Scheme of the nuclear pore complex structure and composition. Asterisks denote dynamic nucleoporins. **(B)** *C. elegans* N2 wild type strain was injected with a vector expressing GFP under the control of either the *ceNup153* promoter or the *ceNup160* promoter (Promoter) or with vectors expressing ceNup153-GFP or ceNup160-GFP under their endogenous promoters (full-length protein). Expression of the reporter protein was analyzed by fluorescence microscopy and GFP signal was merged with differential interference contrast images (DIC). Correct localization of ceNup153-GFP and ceNup160-GFP fusion proteins to the NE was analyzed by confocal microscopy (Zoom). **(C)** The activity of *ceNup153* and *ceNup160* promoters and the localization of full-length proteins in the head of adult worms were analyzed by confocal microscopy. Image shows the maximal projection of 30 z-stacks. **(D)** Nuclei were

purified from ceNup160-GFP and ceNup153-GFP transgenic worms and NPC insertion of the GFP-tagged nucleoporins (green) was confirmed by colocalization with the NPC antibody mAb414 (red). Chromatin is shown in blue. **(E)** ceNup153-GFP and ceNup160-GFP expressing worms were subjected to *GFP* RNAi until no fluorescent signal was detected. RNAi against *C. elegans dicer* (*DCR-1*) was used to release adult worms from the *GFP* RNAi. Adults were fed *DCR-1* RNAi for 6 days before the GFP signal was analyzed. Dashed lines outline worms heads.

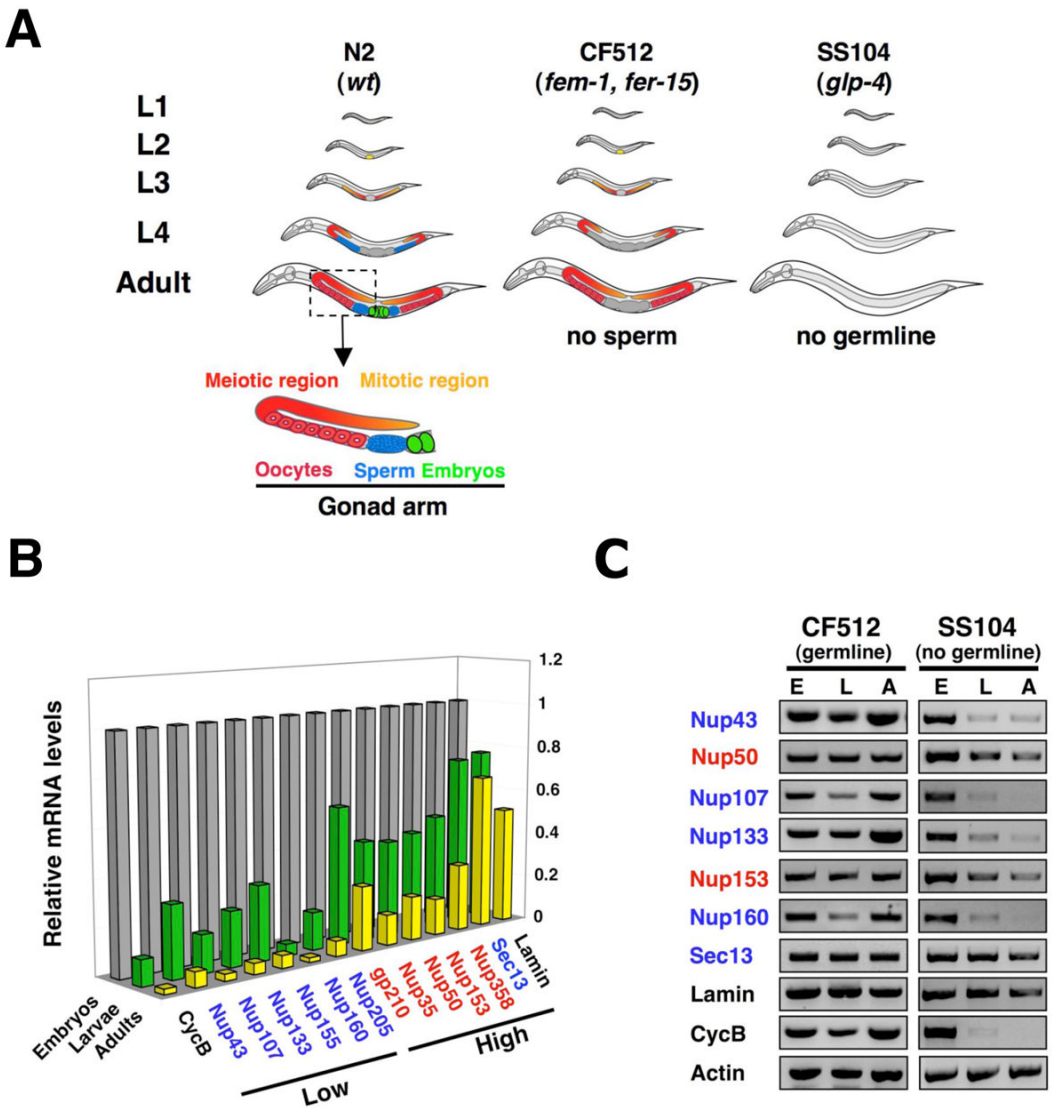


**Figure 2. Expression of scaffold nucleoporins is down-regulated during *C. elegans* development**

**(A)**. Scheme of *C. elegans* strains used in this work (based on (Crittenden et al., 2006)). N2 is wild type strain, CF512 (*fem-1, fer-15*) has thermo-sensitive mutations that inhibit male germline production at 25°C, SS104 (*glp-4*) has a mutation that inhibits male and female germline production at 25°C, being adults worms at the restrictive temperature entirely post-mitotic. **(B)** Total RNA was extracted from the embryo, larva and adult developmental stages of *C. elegans* (SS104 strain). Expression levels were analyzed by RT-PCR (n=4) and normalized to embryonic levels. Cyclin B (CycB) was used as a marker for cell cycle exit. Standard deviation is below 20%. **(C)** Nucleoporin expression levels in embryos (E), larvae (L) and adults (A) worms of *C. elegans* sterile strains CF5120 and SS104 were analyzed by RT-PCR (n=4).

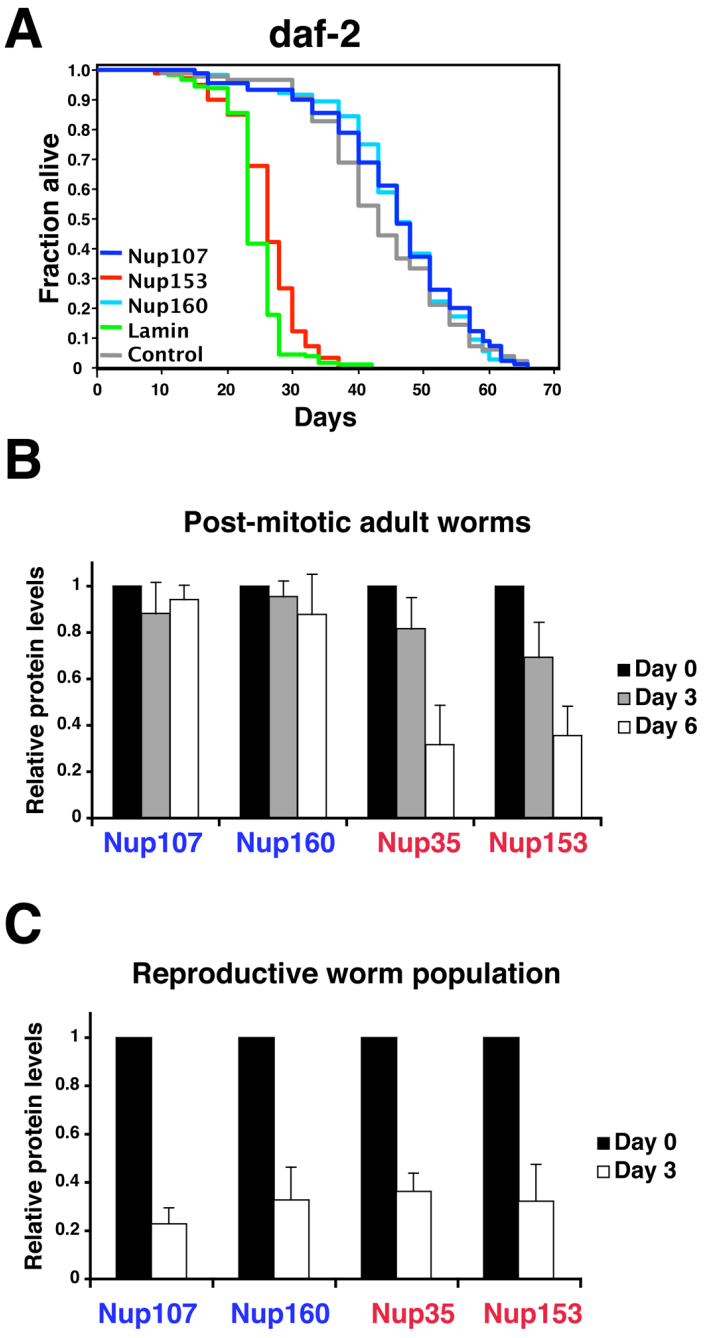


**Figure 3. Expression of scaffold nucleoporins is not required during adulthood**

**(A)**. *daf-2(e1370)* mutant worms on day 1 of adulthood were fed bacteria expressing empty vector control (gray line), *ceNup153* RNAi (red line), *ceNup160* RNAi (light blue line) *ceNup107* RNAi (blue line) or *ceLamin* RNAi (green line). Life span was assessed as described (Apfeld and Kenyon, 1998). Statistical analyses can be found in Table S1. **(B)** Total protein was extracted from sterile (25°C) adults SS104 worms subject to the indicated RNAis for 3 or 6 days and protein levels were assayed by western blot analysis. Values represent average ± SD from 3 independent experiments. **(C)** Total protein was extracted from a reproductive population (15°C) of SS104 worms subjecteded to the indicated RNAis for 3 days and protein

levels were assayed by western blot. Values represent average ± SD from 3 independent experiments.

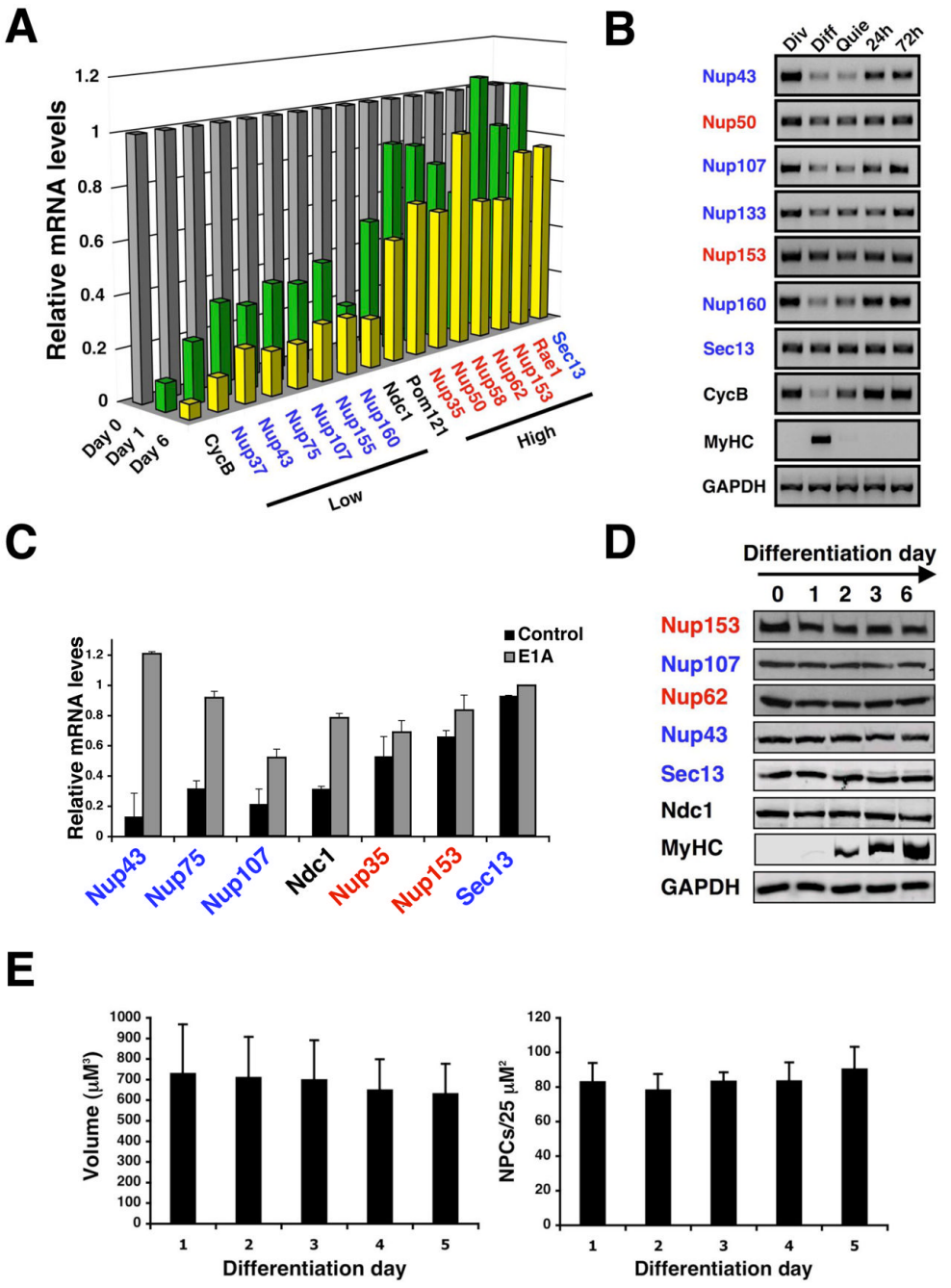


**Figure 4. Down-regulation of scaffold nucleoporin expression is conserved in mammals**

**(A)**. Total RNA was extracted from dividing C2C12 myoblasts (day 0) or differentiated myotubes (day 3 and 6). Nucleoporin expression levels were analyzed by Q-PCR (n=3). Cyclin B was used as a marker for cell cycle exit. In all cases standard deviation is below 20%. **(B)** Total RNA was extracted from dividing (Div), differentiated (Diff) and quiescent (Quie) C2C12 cells. Nucleoporin expression levels were analyzed by RT-PCR. Cyclin B (CycB) and myosin heavy chain (MyHC) were used and controls for cell cycle exit and differentiation respectively. **(C)** Dividing C2C12 myoblasts were infected with retrovirus carrying a control vector or a vector expressing the E1A protein fused to the estrogen receptor. Cells were induced to differentiate for 3–4 days and E1A was activated with 4OH-tamoxifen for 24 hours. Total

RNA was extracted and nucleoporin levels were analyzed by RT-PCR (n=3). **(D)** Total protein was extracted from dividing myoblasts (day 0) or differentiated myotubes (day 1–6). Nucleoporin protein levels during C2C12 differentiation were analyzed by western blotting. Myosin heavy chain (MyHC) was used as a differentiation control. **(E)** C2C12 cells expressing 3GFP-NLS were induced to differentiate. Dividing myoblasts (Day 0) and differentiated myotubes (Day 1–5) were fixed and NPCs were stained using anti-Nup153 antibody. Nuclear volume and NPC density were analyzed by confocal microscopy and quantified.

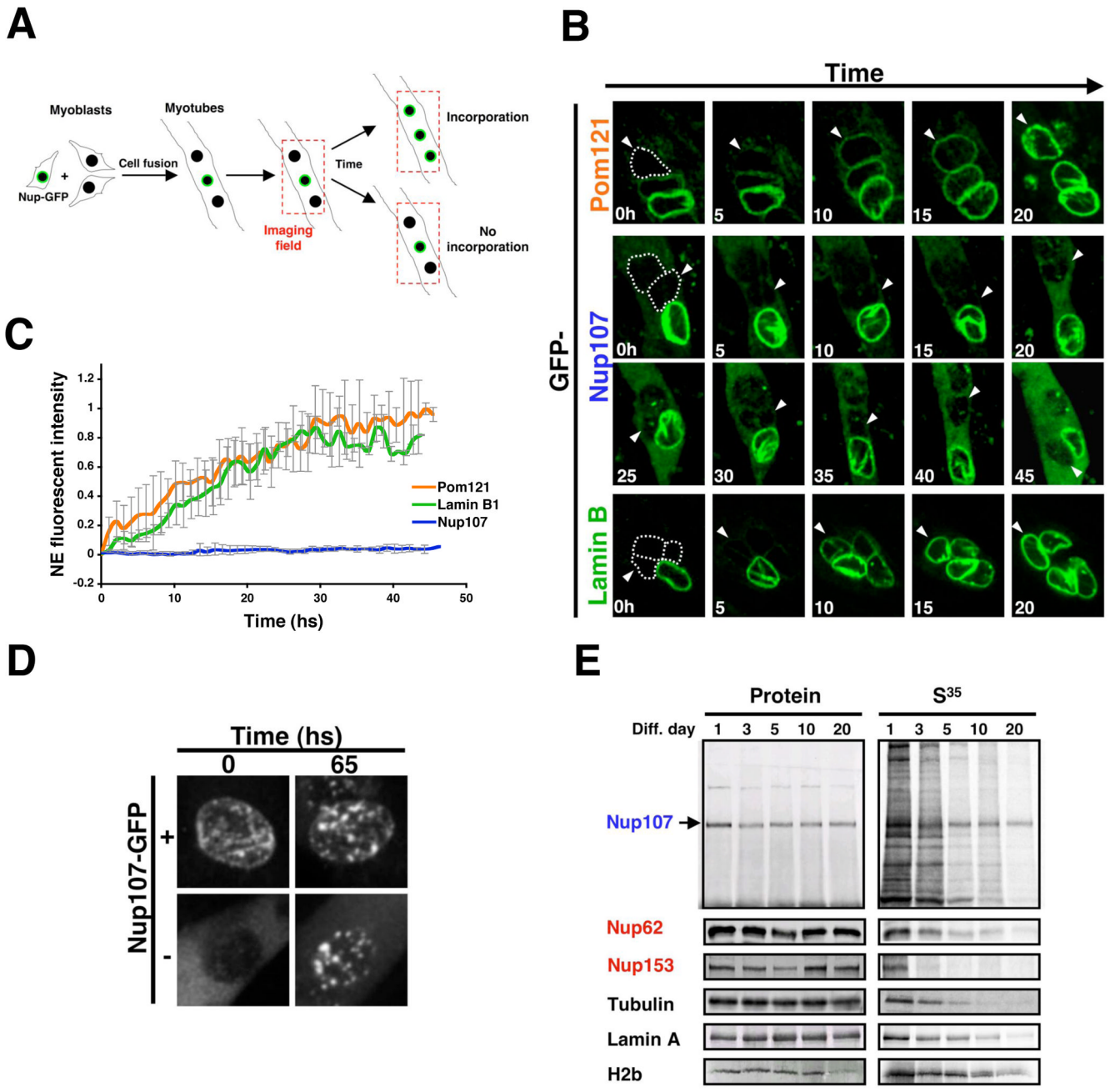


**Figure 5. Nup107 scaffold nucleoporin does not exchange once inserted into NPCs**

**(A)**. Scheme of the imaging setup used to analyze the incorporation of GFP-nucleoporins or Lamin B1-GFP fusion proteins into the NE of differentiated myotubes. **(B)** Proliferating myoblasts were transfected with Pom121-GFP, GFP-Nup107 or Lamin B1-GFP expressing vectors, diluted with untransfected cells and induced to differentiate for 3 days in low serum containing media. Fields containing GFP positive and negative nuclei were selected and imaged using a spinning disk confocal microscope for at least 50 hs at 1 h intervals. Dotted lines show the position of GFP negative nuclei at time 0 and arrowheads are used to follow the GFP negative nuclei during time. **(C)** Incorporation of Pom121-GFP, GFP-Nup107 or Lamin B1-GFP at the NE of GFP negative nuclei was quantified using Image J. **(D)** Proliferating

myoblasts were transfected with a GFP-Nup107 expressing vector, diluted with untransfected cells and induced to differentiate for 3 days. Fields containing nuclei that came from transfected cells (+) or untransfected cells (−) were selected and imaged using a spinning disk confocal. Images show the formation of Nup107 aggregates after 65 hs of overexpression. **(E)** Dividing C2C12 myoblasts were incubated with a $S^{35}$-Methonine/$S^{35}$-Cysteine mix for 24 hs (Pulse) and then switched to differentiating media (Chase). Total cell lysates were prepared from the indicated time points. Proteins were immunoprecipitated using specific antibodies, separated by SDS-PAGE and transfered to nitrocellulose membranes. The presence of $S^{35}$-labeled proteins was analyzed using a phosphoimager and protein levels were determined by western blot.

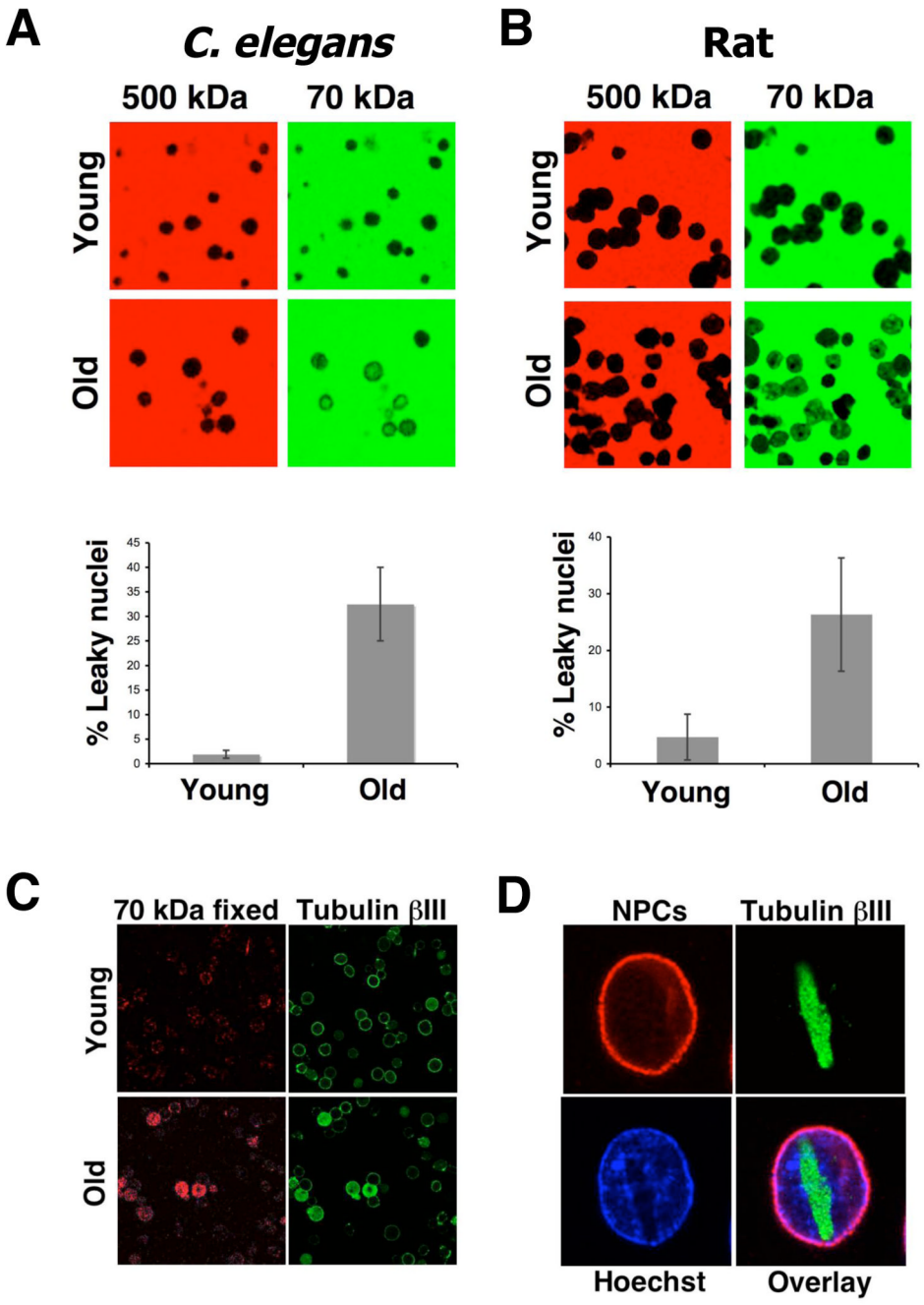


**Figure 6. *C. elegans* and mammals show an age-related increase of nuclear permeability**

**(A)**. Nuclei were isolated from brains of young (3 months) and old (28 months) rats Purified nuclei were incubated with a green 70kDa and a red 500kDa fluorescent dextrans. Nuclear permeability was analyzed by confocal microscopy. Images show each dextran in their original color. The percentage of nuclei that showed influx of the 70kDa dextran was determined using Photoshop CS3 Extended. **(B)**. Nuclei were prepared from *C. elegans* SS104 worms at different times of adulthood. Nuclear permeability was analyzed and quantified as described in (A) **(C)** Young and old rat nuclei were incubated with the 70kDa fluorescent dextran, fixed and stained with an antibody against tubulin bIII. **(F)** Brain nuclei from old rats were fixed and stained with the mAb414 antibody (NPCs) and an anti- tubulin bIII.

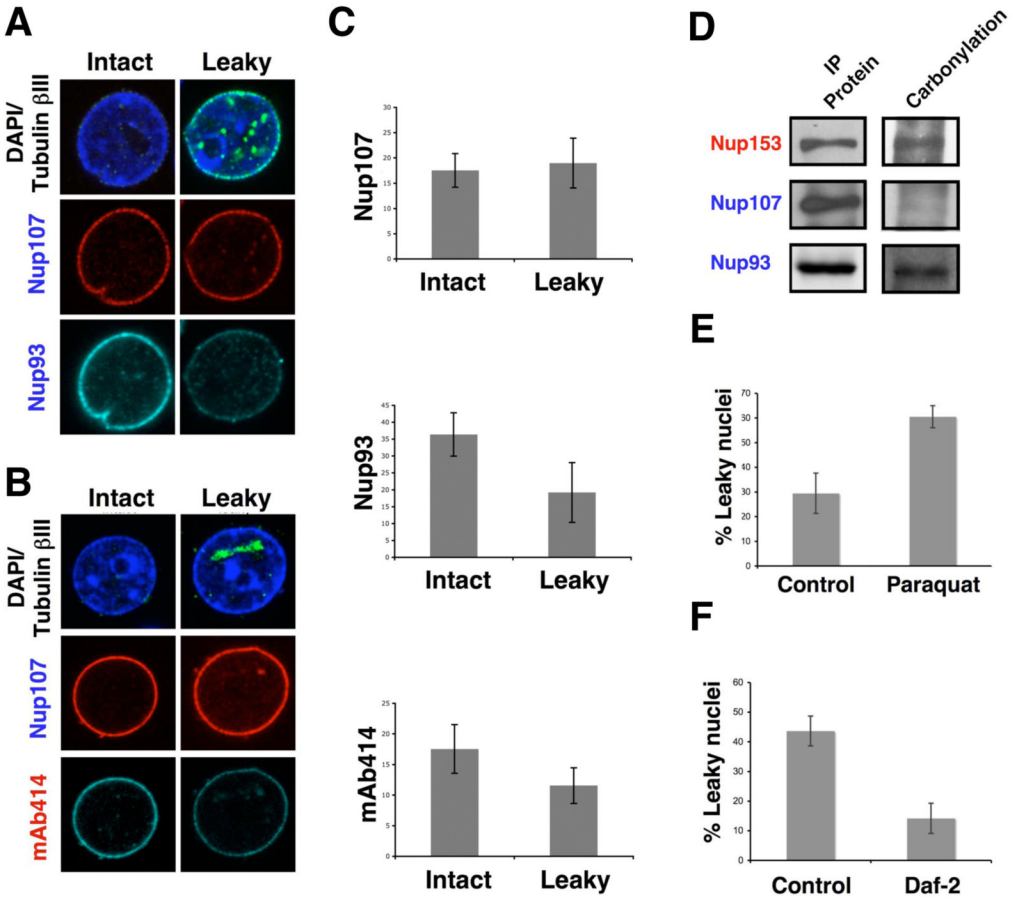


**Figure 7. Nuclei with increase permeability show deteriorated NPCs**

**(A)**. Nuclei were isolated from brains of old (28 months) rats, fixed and stained with antibodies against tubulin bIII and the scaffold nucleoporins Nup107 and Nup133. The staining of intact and leaky nuclei (the latter identified by the intranuclear accumulation of intranuclear tubulin bIII) was compared. **(B)** Intact and leaky nuclei isolated from old rat brains were stained with tubulin bIII, Nup107 and the mAb414 antibody. Intact and leaky nuclei were compared as described in (A). **(C)** The fluorescent intensity of the nuclei stained in (A) and (B) was quantified using Image J. **(D)** Total protein extracts were prepared from brains of old rats and nucleoporins were immunoprecipitated (IP) using specific antibodies. The IP proteins were treated with 2,4-dinitrophenylhydrazine to derivatize carbonyl groups to 2.4-dinitrophenylhydrazone (DNP-hydrazone) The DNP-derivatized proteins were detected by western blot using an anti-DNP antibody. **(E)** C. elegans SS104 worms on day 1 of adulthood were transfer to plates containing bacteria and buffer (Control) or Paraquat (0.5mM). On day 6 nuclei were isolated from worms and nuclear permeability was analyzed using the 70 and 500 kDa dextrans assay and quantified using Photoshop CS3 Extended. **(F)** SS104 adult day 1 worms were grown in bacteria expressing empty vector (Control) or daf-2 RNAi (Daf-2) for 8 days. Nuclei were isolated from worms and nuclear permeability was analyzed as in (D).

## Table 1

Embryonic lethality of *C. elegans* nucleoporin RNAi

| Nucleoporin | *C. elegans gene* | % Embryonic lethality |
|---|---|---|
| Nup35 | *NPP-19* | 92 ± 5 |
| Nup43 | *C09G9.2* | 0 |
| Nup58 | *NPP-4* | 40 ± 9 |
| Nup93 | *NPP-13* | 95 ± 2 |
| Nup107 | *NPP-5* | 0 |
| Nup153 | *NPP-7* | 97 ± 1 |
| Nup160 | *NPP-6* | 94 ± 4 |
| Nup205 | *NPP-3* | 90 ± 6 |
| Lamin | *LMN-1* | 99 ± 1 |

Embryonic lethality: % of hatched embryos ± SD compared to empty vector control (n>3000)